

Faraday Discussions

Accepted Manuscript



This manuscript will be presented and discussed at a forthcoming Faraday Discussion meeting. All delegates can contribute to the discussion which will be included in the final volume.

Register now to attend! Full details of all upcoming meetings: <http://rsc.li/fd-upcoming-meetings>



This is an *Accepted Manuscript*, which has been through the Royal Society of Chemistry peer review process and has been accepted for publication.

Accepted Manuscripts are published online shortly after acceptance, before technical editing, formatting and proof reading. Using this free service, authors can make their results available to the community, in citable form, before we publish the edited article. We will replace this *Accepted Manuscript* with the edited and formatted *Advance Article* as soon as it is available.

You can find more information about *Accepted Manuscripts* in the [Information for Authors](#).

Please note that technical editing may introduce minor changes to the text and/or graphics, which may alter content. The journal's standard [Terms & Conditions](#) and the [Ethical guidelines](#) still apply. In no event shall the Royal Society of Chemistry be held responsible for any errors or omissions in this *Accepted Manuscript* or any consequences arising from the use of any information it contains.

Time resolved in situ X-ray diffraction study of crystallisation processes of large pore nanoporous aluminophosphate materials

Kerry Simmance^{1†}, Wouter van Beek² and Gopinathan Sankar^{1*}

¹Department of Chemistry, University College London, 20 Gordon Street, London WC1H 0AJ, United Kingdom

² Swiss Norwegian Beamline ESRF, F-38000 Grenoble, France

Abstract

Time resolved high-resolution X-ray powder diffraction was utilized to obtain detailed changes in the crystal structure parameters during the hydrothermal crystallization process of nanoporous aluminophosphate AlPO-5 (AFI) structure. This in situ study offered not only the influence of metal ions on the onset of crystallization and estimation of the activation energy of the process, but also allowed us to determine in detail the changes in lattice parameters during this process. More importantly the time-resolved study clearly showed the lattice expansion in the divalent metal ions substituted system right from the on-set of crystallization process, compared to the one without any dopant ions, which suggest that an amorphous or poorly crystalline network is formed prior to crystallization that contains the large divalent ions (compared to Al(III), the substituting element), which is in agreement with the combined XAS/XRD study reported earlier. A mechanism based on this and the earlier study is suggested.

Introduction

Understanding the crystallisation mechanisms taking place during hydrothermal synthesis of open framework zeo-type materials plus the metal substitution mechanism is of considerable interest, since it could lead to a more rational approach towards the design and synthesis of new materials with specific crystalline structure, morphology and particle size for catalytic applications. A large number of studies have been devoted to studying the transformation of gel to nanoporous materials using a variety of *in situ* techniques. However, these studies have, generally, only been able to obtain information on the kinetics of crystallisation (using X-ray diffraction (XRD) methods)^{1, 2}, particle size (through small-angle X-ray scattering (SAXS) techniques)^{3, 4} and local structural change (through X-ray

absorption spectroscopy (XAS))^{4, 5}. Although a combined technique approach using all these methods has been used to derive mechanistic aspects of the crystallisation process^{4, 6}, recent developments, particularly in the area of angular-dispersive High Resolution Synchrotron Powder XRD (HRXRD) (which can also be combined with Raman and XAS)[REF], make it possible to collect high-quality diffraction data in a very short time scale, which will not only determine the kinetics, but also the precise structural parameters, in particular the variation in lattice parameters of the reacting system. To utilise this approach, we investigated the formation of metal substituted nanoporous aluminophosphate catalytic material under hydrothermal conditions.

The family of microporous materials play a very important role in the field of shape selective catalysis and are employed in several industrially important processes, such as methanol to olefin (MTO) conversion^{7, 8}. In the last two decades the development of crystalline microporous materials has been extended to include a variety of other compositions such as aluminophosphates (AIPOs) and metal-organic frameworks (MOFs) as their surface areas and pore volumes are comparable with, if not greater than those of the aluminosilicate zeolites. Discovery of AIPOs dates back to 1982⁹, since then a large range of open-framework aluminophosphate, $\text{AlPO}_4\text{-}n$ (where n denotes a particular structure type), materials have been synthesised.

The structures of $\text{AlPO}_4\text{-}n$ consist of strict alternation of corner sharing Al(III) and P(V) tetrahedra (with a strict framework composition of Al/P = 1) forming an electrically neutral open-framework which unlike aluminosilicate zeolites, requires no extra-framework cations. AIPOs are isoelectronic with SiO_2 . Therefore, in theory, a neutral AIPO framework can be derived from a neutral pure silica zeolite by replacement of two Si(IV) cations with one Al(III) and one P(V) cation. This concept led to the synthesis of a variety of AIPOs by isomorphism substitution of P(V) with Si(IV) to form silicoaluminophosphates (SAPO)¹⁰, or substitution of Al(III) with divalent metal cations, Me(II), which are able to adopt tetrahedral coordination (e.g. Co, Zn, Fe, Mn and Mg) to form metalaluminophosphates (MeAIPO), or with a combination of both to form metalsilicoaluminophosphates (MAPSO)¹¹. This isomorphous substitution renders the framework negative which leads to the AIPO materials having interesting acid and redox catalytic applications.

Furthermore, to be able to synthesise a porous material instead of a dense phase, AIPOs must be synthesised with an organic amine or quaternary ammonium ion, more frequently the former, which acts as a 'structure directing' agent (SDA) or

template. The majority of AlPOs are usually stable upon removal of the organic template and have been found to exhibit thermal stability between 600 and 1000°C.¹² The role which the SDA plays in the formation of the pore dimensions and connectivity is still widely discussed and it has not been possible to assign a distinct attribute of the SDA to its ability to form specific AlPO topologies. Several different purposes of the SDA have been proposed, ranging from it acting purely as a space-filler¹³ to true structure directing.¹⁴

Among the various hetero-atom substituted AlPO's, AlPO-5 (AFI), AlPO-18 (AEI), AlPO-36 (ATS), AlPO-34 (CHA) and AlPO-11 (AEL) have attracted considerable interest due to their ability to induce shape selective catalytic reactions. Within this range of systems, AlPO-5 is one of the most extensively studied, since it has a large pore one-dimensional channel system and more importantly it is the only system which can be prepared in a relatively short time comprising of a range of metal ions (hetero-atoms such as Zn, Co, Mg, Cr, Fe or Mn)^{13, 15, 16} and using a large number of structure directing agents of the type quaternary ammonium salts and amines. For example, this one-dimensional AlPO₄ structure, AlPO-5 can be synthesised using triethylamine (TEA)¹⁷, tripropylamine (TPA)¹⁸, ethyldicyclohexylamine (ECHA)¹⁹ or tetraethylammonium hydroxide (TEAOH). However, most of these organic SDAs only form the AFI topology under very specific conditions. Methyldicyclohexylamine (MCHA), on the other hand, has been shown to only form phase pure AFI over a wide range of synthesis conditions, i.e. pH and temperature²⁰. The AFI framework also shows a high thermal stability during catalysis and it does not collapse upon calcination, when removing the SDA, showing complete integrity^{21, 22}. Therefore, it is of general interest to understand the detailed processes involved in the synthesis of this system, in particular how the metal ions can affect the synthesis process. To do so, it is necessary to use *in situ* techniques that are sensitive to the crystal chemistry, to understand the crystallisation process.

Here, we demonstrate the power of time-resolved HRXRD techniques in understanding the structural changes that takes place during the crystallisation of metal ions substituted aluminophosphate with AFI structure using MCHA as the structure directing agent. The results clearly show that a network containing divalent metal ions along with Al(III) and P(V) are formed prior to the crystallisation process. The study also shows clearly that the lattice parameters are different when metal ions

are incorporated into the framework. Based on this and previous study a mechanism for the formation is proposed.

Experimental

Hydrothermal Synthesis.

The AFI type materials were synthesized by dissolving aluminium hydroxide in an aqueous solution of phosphoric acid. In the case of MeAlPO-5, an aqueous solution of cobalt(II) acetate tetrahydrate (Aldrich) or zinc(II) acetate dihydrate (Aldrich) was also added to the mixture. After rigorous stirring for ca. 10 minutes the gel attains homogeneity and the organic SDA, methylcyclohexylamine (MCHA) (Aldrich), was added to form the final gel which was stirred for ca. 1h.

In situ characterisation.

A gel with composition $(1-x) \text{Al} ; 1.5 \text{P} : x \text{Me} ; 0.8 \text{MCHA} ; 25 \text{H}_2\text{O}$, $x = 0$ or 0.05 , was transferred to a specially designed hydrothermal synthesis cell with an approximate 60% fill volume, and heated to a temperature between 160-170 °C for an appropriate amount of time. Three different gels were studied using synchrotron radiation; unsubstituted AlPO, CoAlPO and ZnAlPO, with the HRXRD study being performed on the BM01B Swiss-Norwegian beamline of the ESRF at a fixed wavelength of 0.5 Å. The details of the beam line and the diffractometer are given elsewhere.²³ The duration of each data collection was tuned with the reaction speed in which the optimized collection period was found to be 2 minutes to cover a 2-theta range of 2-10° (2.89 to 11.89 d-spacing). The data were processed using TOPAS software to extract the lattice parameter of the crystallising system as a function of time.

In a typical experiment, a prepared gel was introduced in to a custom made hydrothermal cell which has a path length of ca 2mm and a window material made of mica (50 micron thick) so that minimum loss of intensity due to cell window and amount of sample in the beam is achieved. The heating bloc was heated to specific temperature before introducing the cell containing gel and the data collection was started once the cell was introduced into the heating block.³ Typically each data collection took approximately 4 minutes.

Results and discussion

Crystallisation of three different precursor gels was monitored by HRXRD (wavelength = 0.5 Å) so that we could study the formation of AlPO-5, Zn-AlPO-5 and Co-AlPO-5 with MCHA as the organic template. In Figure 1 we show stacked plots of the HRXRD data of pure, cobalt and zinc substituted AlPO-5. It is clear from the stacked plots that only phase pure AFI structure is formed, irrespective of the metal content; independent studies at different temperatures, pH of the starting gel and metal content also showed that only AFI structure is formed when MCHA is used as the template implying the true structure-directing aspect of MCHA.²⁴

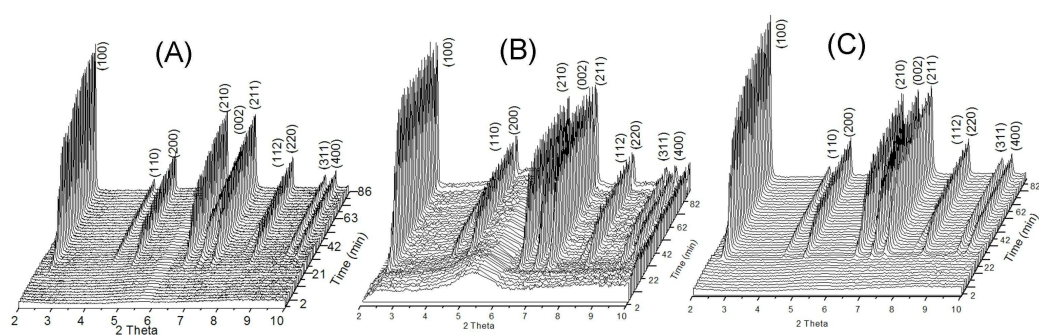


Figure 1. 3D stacked plots of HRXRD patterns collected during the crystallisation, at 170°C, of (A) pure AlPO-5, (B) CoAlPO-5 and (C) ZnAlPO-5. All the reflections are indexed based on the AFI structure and no other phases are seen to form under the experimental conditions. It should be noted that the small amorphous hump observed throughout the synthesis of CoAlPO-5 (B) is due to a higher water amount in the synthesis cell.

The evolution of peak intensities as a function of time can be used to derive valuable information on the kinetics and crystallisation mechanism. The area under the Bragg peaks of each crystalline phase was determined by using a fundamental parameters profile fitting through the TOPAS-*academic* programme²⁵. Comparison of the area under a number of reflections from a single *in situ* experiment revealed crystallisation curves which were generally superimposable over the duration of the experiment, indicating that the growth is isotropic on all crystallographic planes, and therefore all peak areas should be representative of the growth mechanism that takes place during the reaction. For subsequent analysis, the total summed area of all Bragg reflections of each crystalline AFI phase was used; the areas were then converted to the extent of the reaction (α), scaled from 0 to 1, using the relationship $\alpha(t) = I_{hkl}(t) / I_{hkl}(\max)$, where $I_{hkl}(t)$ is the area of a given peak at a given time t and $I_{hkl}(\max)$ is the maximum area of this peak. The resulting sigmoidal crystallisation

curves are shown in Figure 2 and are typical for a crystallisation process consisting of an initial period of induction/nucleation followed by rapid crystallisation of the material and gradual growth of the crystallites until a constant value is reached implying completion of crystal growth.

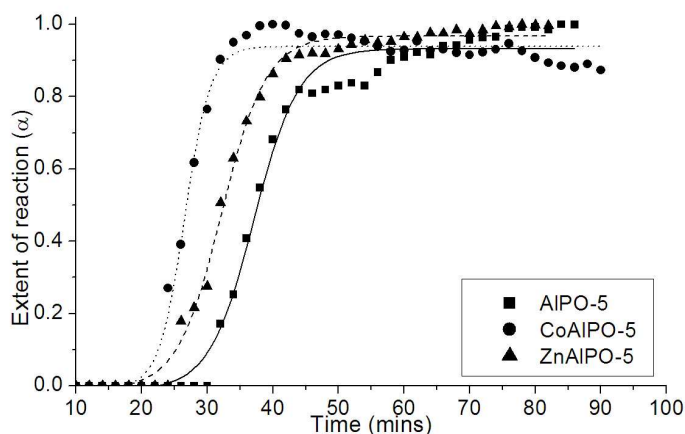


Figure 2. A plot of the crystallisation curves (Boltzmann sigmoid function) of AlPO-5 (■), CoAlPO-5 (●) and ZnAlPO-5 (▲); each point represents the sum of the experimental integrated values of each reflection as a function of time.

These results show that in the presence of a divalent metal cation, in particular Cobalt(II) reduces the induction period compared to unsubstituted AlPO-5, indicating that metal ions (5%) promote the formation of AFI type materials. Similar observations have been made by others¹; however, a previous investigation⁴ on the kinetics of AFI growth contradict our observation, which found that cobalt significantly retards nucleation, growth and crystallisation of this system. Apart from various experimental factors, differences may occur due to the use of triethylamine as the organic template, which can produce more than one phase, unless a specific pH is used for a given metal ion containing system. Another factor, is the metal concentration, which has been found to reverse this trend when the cobalt concentration is above 6 percent¹.

We analysed the HRXRD data in detail to extract the unit cell parameters and crystallite sizes of each crystalline AFI phase employing a fundamental parameters approach using TOPAS-*academic* program²⁵ with the initial unit cell parameters taken from the single crystal X-ray diffraction study of Klap et al.²⁶ ($a(=b) = 13.718 \text{ \AA}$, $c = 8.4526 \text{ \AA}$, $\alpha(=\beta) = 90^\circ$, $\gamma = 120^\circ$ and space group P6/mcc). The results yield interesting additional information on the structural aspects during the growth process. Information on the crystallite size can be obtained from analysis of the full width at half

maximum (FWHM) of the observed diffraction reflections. Figure 3 shows the variation in the crystallite size (Lorentzian component) during the crystallization of AlPO-5, CoAlPO-5 and ZnAlPO-5 as a function of time. Results show that in all three AFI materials, the crystallite size was large at the onset of crystallization, ranging between 80 to 120 nm, and grew by approximately 30 percent during the hydrothermal crystallization.

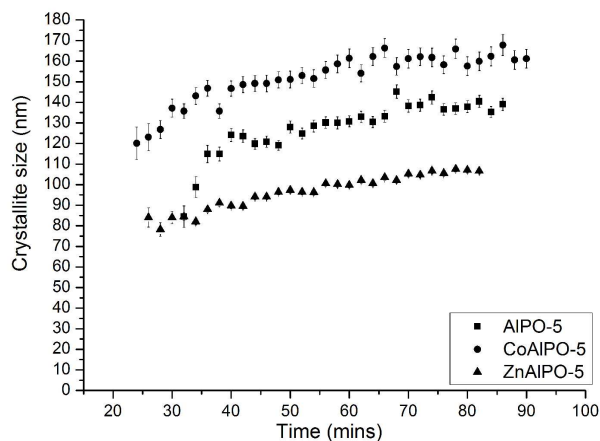


Figure 3. The variation in the crystallite size of the AFI particles is plotted against crystallization time for AlPO-5 (■), CoAlPO-5 (●) and ZnAlPO-5 (▲).

The plots of the $a(=b)$ and c parameters over crystallisation time including the cell volume are shown in Figure 4. The $a(=b)$ parameter remained relatively constant during the crystallisation process and was found to be largest for MeAlPO-5, 13.781 Å (CoAlPO-5) and 13.780 Å (ZnAlPO-5), compared to unsubstituted AlPO-5, 13.735 Å, indicative of the metal cations substituting for aluminium. Tetrahedrally coordinated Co(II) and Zn(II) (direct evidence for the tetrahedral coordination is obtained from respective metal K-edge X-ray absorption spectroscopic data reported elsewhere^{20, 21, 27, 28}) cations have larger ionic radii, 0.58 Å and 0.6 Å respectively, compared to Al(III) which has an ionic radius of 0.39 Å²⁹; therefore an expansion in the $a(=b)$ direction is observed when a metal ion is substituted into the framework. This trend in the $a(=b)$ parameter is in contrast to the c parameter change. The c parameter was found to increase over crystallisation time, more predominantly for unsubstituted AlPO-5 (by approximately 0.02 Å) compared to CoAlPO-5 (increase of 0.01 Å) and ZnAlPO-5 (increase of 0.006 Å).

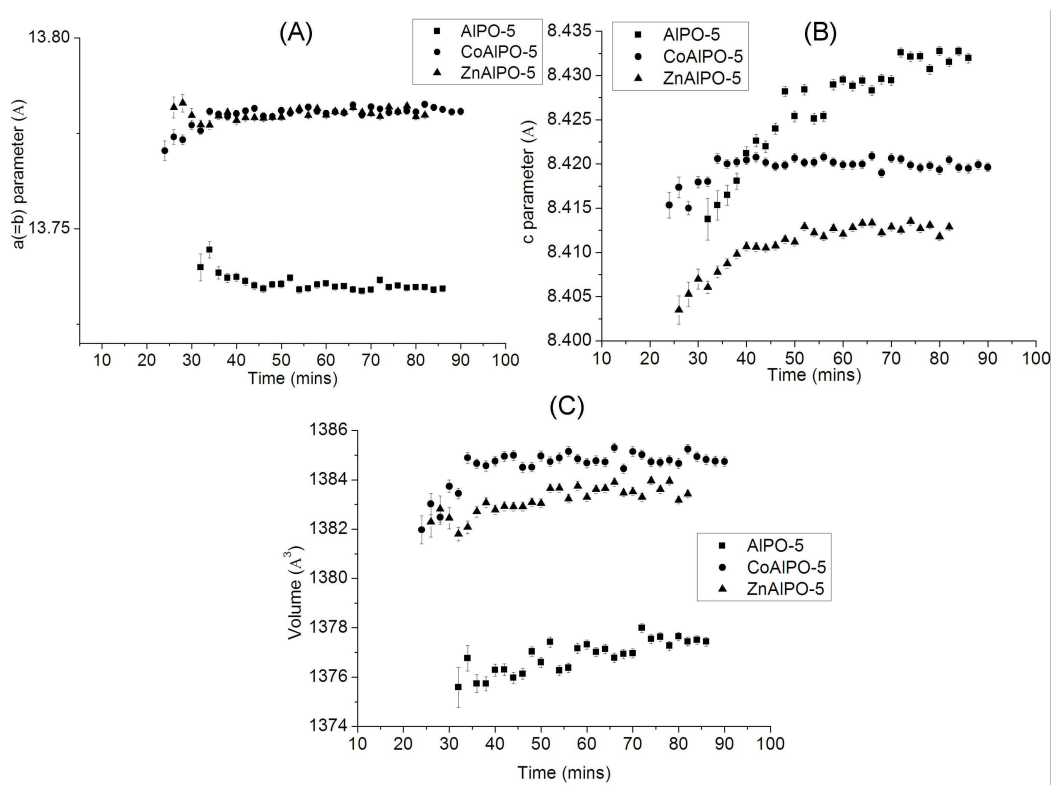


Figure 4. Variation in the lattice parameters obtained from HRXRD data recorded at the BMO1B (SNBL) beam line, as a function of time during the crystallisation of AIPO-5 (■), CoAIPO-5 (●) and ZnAIPO-5 (▲); (A) shows the a(=b) parameter change, (B) the c parameter variation and (C) is the change in the cell volume over crystallisation time. The analysis was performed only on data above ca. 20 minutes, below which the reflections were absent or too few.

The AFI framework is known to have mild hydrophilicity, in which water molecules either bind to framework Al(III) or are physisorbed and reorient isotropically within the channels^{30,31}. Recently, through computational methods it has been shown that water molecules reside in the 6-membered ring channels or, with the organic template, in the 12-membered ring channels pointing in the same direction as crystal growth, the c direction³². Therefore, this increase in the c parameter, over crystallization time, could be due to the uptake of water molecules which may coordinate to Al(III) ions accessible in the channel direction, increasing the Al-O bond distance from 1.74 Å for tetrahedral Al(III) up to 1.9 Å for an octahedral environment; the more hydrophilic pure AIPO-5 material would therefore show a larger increase in the c parameter compared to MeAIPO-5. It should be noted that template orientation within the structure could also play a role in this change in c parameter and cell volume. The uptake of water molecules would also explain the differences seen on comparison of the c parameter at the end of crystallization, in which AIPO-5 was found to have a larger c

parameter compared to MeAlPO-5. XRD patterns collected of the dry as-synthesized forms of these AFI-type materials revealed a *c* parameter decrease with the following trend: MeAlPO-5 > AlPO-5, which is similar to that observed in the *a*(=*b*) parameter. From these findings we can conclude that divalent metal cations, such as Co(II) or Zn(II), are incorporated into the AlPO-5 framework in such a way as to cause an expansion in the *a*(=*b*) direction, which is perpendicular to the channel direction³³. A change in the *c* parameter and cell volume illustrates the flexibility of the AFI framework.

These results provide interesting new information about the crystallisation mechanism of AFI in the presence of divalent metal cations. By combining the information obtained from this *in situ* HRXRD experiment with our previous simultaneous XRD/XAS investigation³³ it is possible to derive a mechanism and a crystallization model for the formation of MeAlPO-5, in particular CoAlPO-5.

Our previous simultaneous XRD/XAS results showed cobalt transforming from octahedral to framework tetrahedral via a pseudo-octahedral intermediate, importantly, the second stage occurred simultaneously with the appearance of Bragg peaks in the diffraction data. This did not agree with previous studies by Grandjean et al.⁴ using *in situ* XAS combined with wide angle X-ray scattering (WAXS) or by Weckhuysen et al.³⁴ using *in situ* UV-Vis, although both studies showed a two-stage transformation of octahedral Co(II) species to tetrahedral Co(II), they reveal Co(II) as tetrahedral species just prior to the onset of crystallization. It is important to note that both these studies referred to above used triethylamine as the organic template, which is well-known to produce a CHA phase as a competing material, under certain conditions³⁵. Although the CHA phase was not observed during the crystallisation process (with the given XRD detection limit), the use of this template may have a different effect on the Co(II) ions. For example, an *ex situ* XRD/Diffuse Reflectance Spectroscopy (DRS) study³⁶ on the formation of MeAlPOs observed a pseudo-octahedral Co(II) species during the formation of CoAlPO-5 (AFI). However, this species was not present during the formation of CoAlPO-34 (CHA).

Therefore by combining the findings from our previous simultaneous XRD/XAS investigation with our recent *in situ* HRXRD study; results suggest that CoAlPO-5 material is formed via a solid hydrogel transformation mechanism. In this mechanism it is believed that the structure of the molecular sieve material is obtained by reorganization of the framework of solid phase aluminophosphate hydrogel formed

from the condensation of phosphate and aluminate ions in the early stages of crystallization³⁷. The crystallographic $a(=b)$ parameter is large even at the onset of phase formation (compared to un-substituted AlPO-5) and remained constant throughout the reaction, indicating that the cobalt(II) ions are part of the solid-phase network prior to crystallization and it is unlikely the Co(II) ions are incorporated into the structure from solution phase. This is also supported by evaluation of the crystallite size over time, which revealed the formation of large particles at the onset of crystallization.

A schematic illustration of the mechanism of formation and substitution of cobalt(II) into the AFI structure is given in Figure 5. It is generally accepted that the synthesis gel consists of AlO_4 and PO_4 tetrahedrons which form a 1D chain unit³⁸⁻⁴¹ along with a $[\text{Co}(\text{H}_2\text{O})_6]^{2+}$ species. The octahedral Co(II) transforms to a $[\text{CoO}_4(\text{H}_2\text{O})_2]^{2+}$ or $[\text{CoO}_5(\text{H}_2\text{O})]^{2+}$ species, in which some of the coordinating oxygen atoms bridge between two cations (P(V)-O-Co(II)). At the onset of crystallization, Co(II) ions start to lose the bound water molecules to form a tetrahedral environment and, simultaneously, water molecules bind to Al(III) ions accessible in the channels. The majority of these water molecules bound to the Al(III) ions are then lost upon dehydration of the solid. A solid hydrogel transformation mechanism and similar phenomena have previously been observed in zeolite and aluminophosphate synthesis⁴² In relation to other divalent metal substituted AFI materials, such as ZnAlPO-5, the unit cell parameters were found to have the same trend over crystallization time, indicating a similar mechanism of formation. Although, XAS does not provide additional supporting information on the zinc ion incorporation, Zn(II) ions adopt a tetrahedral coordination environment in the synthesis gel. This study has shown that HRXRD can be a very powerful tool in elucidating information on the crystallization mechanism.

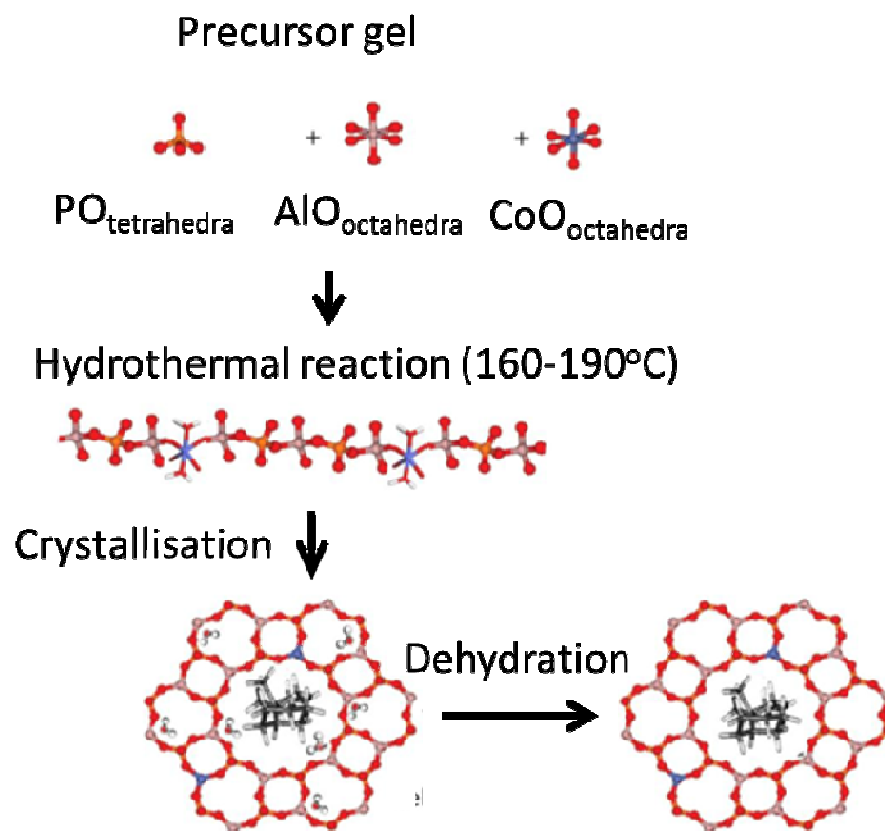


Figure 5. A schematic illustration of the formation of CoAlPO-5 based on our combined X-ray absorption spectroscopy at the Co K-edge and X-ray diffraction studies reported here and elsewhere. Co(II) = blue, P(V) = orange, Al(III) = light pink, O = red, H = white. The organic template is shown in grey scale.

Summary

In this study, we have determined not only the kinetics using time-resolved angular dispersive HRXRD, but also the structural parameters, in particular the variation in lattice constants, during the hydrothermal synthesis of AFI type materials. By combining results from our previous *in situ* simultaneous XRD/XAS (reported elsewhere) with this *in situ* high-resolution XRD study we propose that the crystallisation of CoAlPO-5 may occur via a solid hydrogel transformation mechanism. In this mechanism it is believed that the structure of the molecular sieve material is obtained by reorganisation of the framework of solid phase aluminophosphate hydrogel formed from the condensation of phosphate and aluminate ions in the early stages of crystallisation⁴³. The crystallographic $a(=b)$ parameter is large even at the onset of phase formation (compared to unsubstituted

AlPO-5) and remained constant throughout the reaction, indicating that the divalent metal ions are part of the solid-phase network (amorphous or poorly crystalline solid) formed prior to the crystallisation process and it is unlikely that the divalent ions are incorporated into the structure from solution phase.

Acknowledgements

We thank the EPSRC and Royal Society (to GS) for their financial support and ESRF for the provision of beam time and other facilities.

References

1. A. T. Davies, G. Sankar, C. R. A. Catlow and S. M. Clark, *Journal of Physical Chemistry B*, 1997, 101, 10115-10120.
2. G. Sankar, T. Okubo, W. Fan and F. Meneau, *Faraday Discussions*, 2007, 136, 157-166.
3. G. Sankar and W. Bras, *Catalysis Today*, 2009, 145, 195-203.
4. D. Grandjean, A. M. Beale, A. V. Petukhov and B. M. Weckhuysen, *Journal of the American Chemical Society*, 2005, 127, 14454-14465.
5. M. Dong, G. F. Wang, Z. F. Qin, J. G. Wang, T. Liu, S. P. Yuan and H. J. Jiao, *Journal of Physical Chemistry A*, 2007, 111, 1515-1522.
6. G. Sankar, J. M. Thomas, F. Rey and G. N. Greaves, *Journal of the Chemical Society-Chemical Communications*, 1995, 2549-2550.
7. G. Bellussi and P. Pollesel, in *Molecular Sieves: from Basic Research to Industrial Applications, Pts A and B*, eds. J. Cejka, N. Zilkova and P. Nachtigall, 2005, vol. 158, pp. 1201-1212.
8. J. M. Thomas, R. Raja, G. Sankar and R. G. Bell, *Accounts of Chemical Research*, 2001, 34, 191-200.
9. S. T. Wilson, B. M. Lok, C. A. Messina, T. R. Cannan and E. M. Flanigen, *Journal of the American Chemical Society*, 1982, 104, 1146-1147.
10. B. M. Lok, C. A. Messina, R. L. Patton, R. T. Gajek, T. R. Cannan and E. M. Flanigen, *Journal of the American Chemical Society*, 1984, 106, 6092-6093.
11. E. M. Flanigen, B. M. Lok, R. L. Patton and S. T. Wilson, *Pure and Applied Chemistry*, 1986, 58, 1351-1358.
12. J. Yu and R. Xu, *Chemical Society Review*, 2006, 35, 593.
13. S. T. Wilson and E. M. Flanigen, *Acs Symposium Series*, 1989, 398, 329-345.
14. M. G. O'Brien, M. Sanchez-Sanchez, A. M. Beale, D. W. Lewis, G. Sankar and C. R. A. Catlow, *Journal of Physical Chemistry C*, 2007, 111, 16951-16961.

15. I. Arends, R. A. Sheldon, M. Wallau and U. Schuchardt, *Angewandte Chemie-International Edition in English*, 1997, 36, 1144.
16. M. Hartmann and L. Kevan, *Chemical Reviews*, 1999, 99, 635-663.
17. Y. Liu, R. L. Withers and L. Noren, *Solid State Sciences*, 2003, 5, 427-434.
18. O. Weiss, G. Ihlein and F. Schuth, *Microporous and Mesoporous Materials*, 2000, 35-6, 617-620.
19. J. M. Bennett, J. P. Cohen, E. M. Flanigen, J. J. Pluth and J. V. Smith, *Acs Symposium Series*, 1983, 218, 109-118.
20. M. Sanchez-Sanchez, G. Sankar, A. Simperler, R. G. Bell, C. R. A. Catlow and J. M. Thomas, *Catalysis Letters*, 2003, 88, 163-167.
21. P. A. Barrett, G. Sankar, C. R. A. Catlow and J. M. Thomas, *Journal of Physical Chemistry*, 1996, 100, 8977-8985.
22. G. Sankar, R. Raja and J. M. Thomas, *Catalysis Letters*, 1998, 55, 15-23.
23. E. Boccaleri, F. Carniato, G. Croce, D. Viterbo, W. van Beek, H. Emerich and M. Milanese, *Journal of Applied Crystallography*, 2007, 40, 684-693.
24. G. J. Klap, H. van Koningsveld, H. Graafsma and A. M. M. Schreurs, *Microporous and Mesoporous Materials*, 2000, 38, 403-412.
25. A. A. Coelho, 2007.
26. W. B. Fan, B. B. Fan, M. G. Song, T. H. Chen, R. F. Li, T. Dou, T. Tatsumi and B. M. Weckhuysen, *Microporous and Mesoporous Materials*, 2006, 94, 348-357.
27. P. A. Barrett, G. Sankar, R. H. Jones, C. R. A. Catlow and J. M. Thomas, *Journal of Physical Chemistry B*, 1997, 101, 9555-9562.
28. G. Sankar, G. Muncaster, D. Gleeson, C. R. A. Catlow, J. M. Thomas, J. F. W. Mosselmanns, I. Harvey and A. J. Dent, *Journal of Synchrotron Radiation*, 2001, 8, 622-624.
29. D. B. Akolekar, *Applied Catalysis a-General*, 1998, 171, 261-272.
30. D. Goldfarb, H. X. Li and M. E. Davis, *Journal of the American Chemical Society*, 1992, 114, 3690-3697.
31. R. S. Pillai and R. V. Jasra, *Langmuir*, 2010, 26, 1755-1764.
32. L. Gomez-Hortigueela, J. Perez-Pariente and F. Cora, *Chemistry-a European Journal*, 2009, 15, 1478-1490.
33. K. Simmance, G. Sankar, R. G. Bell, C. Prestipino and W. van Beek, *Physical Chemistry Chemical Physics*, 12, 559-562.
34. B. M. Weckhuysen, D. Baetens and R. A. Schoonheydt, *Angewandte Chemie-International Edition*, 2000, 39, 3419-+.
35. F. Rey, G. Sankar, J. M. Thomas, P. A. Barrett, D. W. Lewis, C. R. A. Catlow, S. M. Clark and G. N. Greaves, *Chemistry of Materials*, 1995, 7, 1435-1436.
36. B. M. Weckhuysen, R. R. Rao, J. A. Martens and R. A. Schoonheydt, *European Journal of Inorganic Chemistry*, 1999, 565-577.
37. R. R. Xu, P. Wenqin, J. H. Yu, H. Qisheng and J. Chen, *Chemistry of Zeolites and Related Porous Materials - Synthesis and Structure*, John Wiley and sons Ltd, Singapore, 2007.
38. B. A. Adair, S. Neeraj and A. K. Cheetham, *Chemistry of Materials*, 2003, 15, 1518-1529.
39. A. A. Ayi, S. Neeraj, A. Choudhury, S. Natarajan and C. N. R. Rao, *Journal of Physics and Chemistry of Solids*, 2001, 62, 1481-1491.

40. A. M. Beale, A. M. J. van der Eerden, D. Grandjean, A. V. Petukhov, A. D. Smith and B. M. Weckhuysen, *Chemical Communications*, 2006, 4410-4412.
41. J. H. Yu and R. R. Xu, *Accounts of Chemical Research*, 2003, 36, 481-490.
42. W. Y. Xu, J. Q. Li, W. Y. Li, H. M. Zhang and B. C. Liang, *Zeolites*, 1989, 9, 468-473.
43. P. Xu, W. Pang, Q. Huo and J. Chem, *Chemistry of Zeolites and Related Porous Materials - Synthesis and Structure*, John Wiley and sons Ltd., Singapore, 2007.